Statistical approach of chemistry and topography effect on human osteoblast adhesion

Sylvain Giljean, Arnaud Ponche, Maxence Bigerelle, Karine Anselme

Statistical approach of chemistry and topography effect on human osteoblast adhesion

S. Giljean,[1,2] A. Ponche,[1] M. Bigerelle,[3,4] K. Anselme[1,5]

[1]Institut de Science des Matériaux de Mulhouse (IS2M), CNRS LRC7228, Université de Haute-Alsace, 15 rue Jean Starcky, BP 2488, 68057 Mulhouse Cedex, France
[2]Équipe MMPF-Pôle STIC-SPI Maths, IUT de Mulhouse Département GMP, Université de Haute-Alsace, 61 rue Albert Camus, 68093 Mulhouse cedex, France
[3]Équipe Matériaux ENSAM Lille - Laboratoire de Métallurgie Physique et de Génie des Matériaux, CNRS UMR 8517, 8 Boulevard Louis XIV, 59046 Lille, France
[4]Laboratoire Roberval, Université de Technologie de Compiègne, Centre de Recherches de Royallieu, CNRS UMR 6253, BP 20529, 60205 Compiègne cedex, France
[5]Laboratoire de Recherche sur les Biomatériaux et les Biotechnologies, Université du Littoral Côte d'Opale, 52 rue du Dr Calot, 62608 Berck sur mer cedex, France

Abstract: Our objective in this work was to determine statistically the relative influence of surface topography and surface chemistry of metallic substrates on long-term adhesion of human bone cell quantified by the adhesion power (AP). Pure titanium, titanium alloy, and stainless steel substrates were processed with electro-erosion, sandblasting, or polishing giving various morphologies and amplitudes. The surface chemistry was characterized by X-ray photoelectron spectroscopy (XPS) associated with an extensive analysis of surface topography. The statistical analysis demonstrated that the effect on AP of the material composition was not significant. More, no correlation was found between AP and the surface element concentrations determined by XPS demonstrating that the surface chemistry was not an influencing parameter for long-term adhesion. In the same way, the roughness amplitude, independently of the process, had no influence on AP, meaning that roughness amplitude is not an intrinsic parameter of long-term adhesion. On the contrary, the elaboration process alone had a significant effect on AP. For a same surface elaboration process, the number of inflexion points, or *G* parameter, was the most pertinent roughness parameter for describing the topography influence on long-term adhesion. Thus, more the inflexion points, more the discontinuities, higher the long-term adhesion.

Key Words: surface chemistry, topography, titanium, stainless steel, adhesion, osteoblast

INTRODUCTION

Surface topography of bone implants are often modified using various processes (plasma-spraying, sandblasting, machining, etc.) to improve their osseointegration. The efficiency of these processes has been demonstrated in several *in vivo* experiments.[1–4] Alternatively, many *in vitro* studies have been performed to understand how cells respond to surface topography. The surface roughness has been shown to critically influence the cell adhesion.[5–10] However, other studies have also claimed that the surface chemistry is the main influencing factor on cell adhesion.[11–18]

The relative influence on cell adhesion of surface topography and surface chemistry is relatively difficult to elucidate as it is extremely difficult to control one factor without changing the other. More frequently, the authors tried to apply the same processes to different materials to compare the cell adhesion on substrates with same topography but different chemistries. However, it has been demonstrated that the process used to increase surface roughness can completely disturb the surface chemistry of a titanium alloy (V).[19] To get round these problems and to be able to discriminate the relative effects of chemistry and roughness, Wieland et al. proceeded to the preparation of epoxy-resin replicas of titanium substrates with various rough topographies.[20] These replicas were then tested in culture with fibroblastic cells. Alternatively, we compared the adhesion of human osteoblasts on pure titanium (T) and V rough surfaces covered or not by a thin gold–palladium layer with the aim to check if the adhesion was different on surfaces with the same topographies but with different chemistries.[6,21] We demonstrated that the topography was the main influencing factor on cell response. This was confirmed recently by other authors using fibroblastic cells.[22] Hacking et al. applied the same process on implants and

Correspondence to: K. Anselme; e-mail: karine.anselme@uha.fr
Contract grant sponsor: CETIM (Centre Technique des Industries Mécaniques) Foundation, Senlis, France (Nouvelles Méthodes D'analyse des états de Surfaces : de la Caractérisation à la Recherche de Paramètres Pertinents)

demonstrated *in vivo* that hydroxyapatite plasma-sprayed implants covered by a thin titanium mask displayed the same osseointegration than non covered implants demonstrating that the most significant parameter on osseointegration of these implant was their surface morphology and not their surface chemistry.[23]

Some studies have been published on the relative influence of surface chemistry and roughness on cell response[19,24–30] but very rarely these analysis were supported by statistical analysis.[31] Our objective in this study is to compare statistically the adhesion of human osteoblasts on T, V, and stainless steel 316L (I) substrates processed with electro-erosion, sandblasting, or polishing giving various morphologies and amplitudes. An extensive analysis of topography of all the substrates will be performed and more than hundred parameters will be computed. The surface chemistry will be characterized by X-Ray photoelectron spectroscopy (XPS). The adhesion of human osteoblasts will be quantified by their adhesion power (AP) as previously described.[32–34] Finally, multivariate analysis of variance studies will be performed to determine how the AP of cells is influenced by surface topography and surface chemistry.

MATERIALS AND METHODS

Surface preparation

V, T, or I (supplied by Acnis International, Villeurbanne, France) were processed to obtain various surface morphologies. V, T, and I bars (14, 12, and 10 mm in diameter, respectively) were machine-tooled to obtain samples measuring 2 mm in thickness. The samples were polished (VP, TP, IP) using a Pedemax 2 automatic polishing machine (Struers S.A.S, Champigny sur Marne, France) and grade 40 silicon carbide paper. The three different materials were also sandblasted (SB) using silicon carbide particles measuring 120 or 400 μm in diameter to obtain substrates with two roughness amplitudes (level 0 or level 1) named respectively VS0, TS0, IS0 and VS1, TS1, IS1. Lastly, the three different materials were electro-eroded (EE) using an electro-erosion cutting machine (Wire machine-tooling AGIECUT, Premier Equipment, Altamonte Springs, FL, USA) under two different conditions to obtain substrates with two different roughness amplitudes (level 0 or level 1) named, respectively, VE0, TE0, IE0 and VE1, TE1, IE1. The first ones were cut at 3 A and then the tooled face was EE twice at 0.25 A. The second ones were cut at 3 A and then the tooled face was EE twice more at decreasing powers (1 and 0.25 A).

The surface morphologies of these different surfaces are illustrated in Figure 1.

Roughness measurement

Roughness was measured using a tactile profilometer (Tencor P10) on a surface of 1×1 mm^2 with one measure each 2 μm on horizontal and vertical scanning. Three-dimensional profiles were drawn and analyzed on a computer using personal software.

A hundred roughness parameters were computed. Classical roughness amplitude parameters were used like Ra, Rk, and Rt. Frequency roughness parameters were also analyzed like the autocorrelation length (LAC), the number of peaks per inch of the profile or the *G* parameter which represents the ratio of inflexion points on a length of profile (see Appendix). An inflexion point is a point on a curve at which the curvature changes sign. The curve changes from being concave upwards (positive curvature) to concave downwards (negative curvature) or vice versa.

X-ray photoelectron spectroscopy

XPS analysis was performed on a Gammadata Scienta (Uppsala, Sweden) SES 200-2 X-ray photoelectron spectrometer under ultrahigh vacuum ($p < 10^{-9}$ mbar). The monochromatized AlKα source (1486.6 eV) was operated at a power of 420 W (30 mA and 14 kV) and the spectra were acquired at a take-off angle (TOA) of 90° (angle between the sample surface and photoemission direction). The samples were outgassed in several ultrahigh vacuum chambers with isolated pumping systems and pressure control until transfer to the analysis chamber. During acquisition, the pass energy was set to 500 eV for wide scans and to 100 eV for high-resolution spectra. Classical Scofield sensitivity factors were used for peak fitting procedures with CASAXPS software (Casa Software, Teignmouth, UK, www.casaxps.com). All line shapes used in peak fitting procedures were a mix of 30% Gaussian and 70% Lorentzian. To limit errors on background determination due to low signal-to-noise ratio, the two limit points of the Shirley-type background have been averaged on 21 experimental points. All components on high-resolution spectra were referenced according to the CH_x component at 285.0 eV.

Cell culture

Human osteoblasts were obtained from trabecular bone taken from the iliac crest of young patients after the positive decision of the local ethic committee. Cells were initially cultured in Dulbecco Modified Essential Medium (DMEM, Eurobio, France) containing 10% fetal bovine serum, 100 units/ml of penicillin, and 100 μg/ml of streptomycin, until confluence and were then preserved in liquid nitrogen in complete DMEM + 10% dimethylsulfoxyde (Sigma, L'Isle d'Abeau, France) for several months. The cells were then thawed and cultured in 75-cm^2 flasks. At confluence, the cells were harvested using trypsin–EDTA and inoculated onto samples in 24-well plates for adhesion tests. The medium was changed twice a week.

Adhesion measurement

Samples of each surface were inoculated with 4×10^4 cells/sample. In each experiment, three samples were analyzed after each incubation period: 24 h, 7 days, 14 days, and 21 days. The cells were enzymatically detached from the samples by a diluted trypsin–EDTA (0.025% v/v) treatment as previously described.[35] Briefly, cells detached after 5, 10, 20, 30, and 60 min of contact with the diluted enzyme were counted. At the end, the remaining cells were detached by two successive final 15-min treatment with nondiluted trypsin–EDTA. The number of released cells

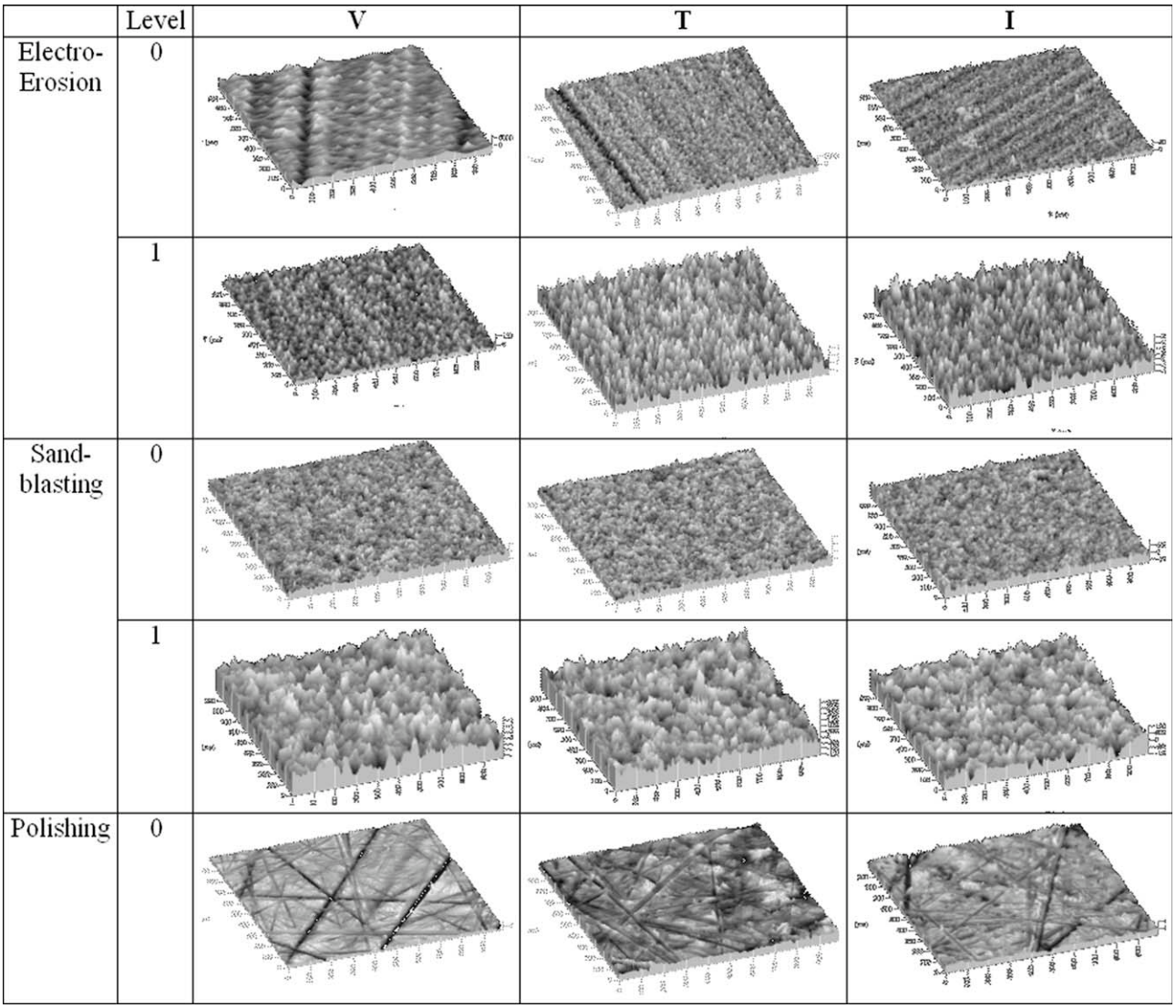

FIGURE 1. 3D images obtained by contact profilometry of Ti6Al4V (V), pure titanium (T), and stainless steel (I) surfaces.

versus trypsination time were established. These experiments were done at least in triplicate. Thus, at least nine measurements were obtained for each of the 15 different surfaces and finally more than 2500 numerical values were treated statistically.

There exists an experimental bias in the measure of adhesion of a cell population cultured on a substrate during 21 days. Indeed, after 21 days culture, the cell number includes both the initial deposited cells and cells that have proliferated. As a consequence, we have developed a mathematical function that permits to decorrelate each cell number. The method was fully developed and published by our team in other papers.[36,37] This method permits to characterize the cell adhesion by the AP. We have previously demonstrated that the AP represents the strength of the cell–material interface formed during 3 weeks of culture, involving at once the extracellular matrix proteins synthesized by the cells themselves and the cell–cell contacts.[32,35]

Scanning electron microscopy

Before culture, samples were sputter-coated (Emscope SC 500, Elexience, Paris, France) and examined using a Hitachi S520 scanning electron microscope at an accelerating voltage of 25 kV (Elexience, Paris, France).

After culture, cell layers were fixed, rinsed, dehydrated in graded alcohol, critical-point dried with CO_2 (Emscope CPD 750, Elexience, Paris, France), sputter-coated (Emscope SC 500, Elexience, Paris, France), and examined using a Hitachi S520 scanning electron microscope at 25 kV (Elexience, Paris, France) or using a Philips SEM 525M at 30 kV (FEI, Limeil-Brevannes, France).

Statistical analysis

Three statistical tools were used. The classical analysis of variance (ANOVA) was used to test the influence on AP of materials, level of roughness amplitude and the process

TABLE I. Roughness Values of the Different Samples Tested

Material	Process	Roughness Amplitude (Level)	Name	Ra (μm)	Rt (μm)	LAC (μm)	Peaks	*G*
Ti6Al4V alloy	Electro-erosion	0	VE0	1.07	8.0	12.2	606	0.1640
		1	VE1	2.25	15.5	11.0	612	0.1621
	Sand-blasting	0	VS0	0.81	6.6	10.2	801	0.1610
		1	VS1	2.43	17.0	17.5	454	0.1681
	Polishing	–	VP	0.36	3.0	18.9	433	0.1676
Pure titanium	Electro-erosion	0	TE0	0.76	6.2	9.2	753	0.1624
		1	TE1	2.52	16.0	11.3	600	0.1610
	Sand-blasting	0	TS0	0.86	6.9	11.8	764	0.1621
		1	TS1	2.29	16.5	18.4	456	0.1683
	Polishing	–	TP	0.53	4.5	21.1	452	0.1686
Stainless steel	Electro-erosion	0	IE0	0.81	6.2	9.9	824	0.1636
		1	IE1	2.55	16.8	12.2	575	0.1652
	Sand-blasting	0	IS0	0.79	6.5	9.3	845	0.1626
		1	IS1	2.08	14.4	16.5	485	0.1671
	Polishing	–	IP	0.60	5.5	15.6	546	0.1692

used to create the surface as well as the interaction between the process and the roughness amplitude. The marginal (type III) sums of squares was used since they correspond to the variation attributable to an effect after correcting for any other effects in the model. They are unaffected by the frequency of observations. To test if a correlation existed between AP and surface chemical composition determined by XPS, linear model was applied and *t* value was computed to analyze if the slope was significant at a *p* level of 5%.

RESULTS

The samples with a roughness level 0 (fine roughness) had an Ra of 0.85 ± 0.11 μm and the samples with a roughness level 1 (coarse roughness) an Ra of 2.35 ± 0.18 μm. The polished samples had an Ra of 0.50 ± 0.12 μm (Table I).

Surface analysis

Surface topography. The electro-erosion produced relatively rough surfaces with a melted aspect presenting sheets with smooth edges associated with some globules. The SB surfaces presented the well-known rough surfaces with depression and indentations among flatter appearing areas of various sizes. The polished surfaces presented defect lines created by polishing with various depth, width, and orientation (Fig. 1). Whatever the process used to produce roughness, no difference was observed in resulting surface morphology on the three different materials.

Surface composition. XPS analysis was performed on all samples and allowed to monitor the atomic surface composition of each sample as presented in Table II. To consider the element percentage without considering the atmospheric contamination layer, the atomic concentration was obtained after deduction of the carbon and oxygen components and then the other elements were normalized to 100% (Table II, numbers in bracket). A part of the elements found are related to contamination by processing. On EE samples, signals of zinc and copper were measured demonstrating a contamination by elements from wire of the electro-erosion cutting machine surely "buried" in the oxide film when removing the samples from water. On SB surfaces, a foreseeable contamination by silicon was observed surely linked to the inlaying of silicon carbide particles in the surface oxide layer during polishing preceding the sand blasting. This result is confirmed with a foreseeable contamination by silicon on polished surfaces. On SB surfaces, a contamination of the surface during the process by the alumina particles (10–12%) can also be noted. A non negligible calcium contamination (about 1%) from tap water was also found on T and V surfaces. All samples also present a small part of nitrogen (1–4%) probably due to manipulations of samples by research workers. Sulfur is randomly observed on four different samples without explanation regarding the process. Concerning I samples, original presence of chromium, phosphorus, and manganese from the bar is conserved after each process. Whatever the samples, oxygen rise from 21 to 35% while carbon level rise from 36 to 71%. It can be noted that polished surfaces have the lowest oxygen level and the highest carbon level for the three materials surely related to contamination by lubricating fluids and oils.[38]

The metallic titanium is in the range 1–6% according to the process. The low concentration of the metallic Ti is correlated with the high amount of ubiquitous hydrocarbons adsorbed from the atmosphere and to the oxide layer covering the titanium surface. Thus, the maximum theoretical amount of titanium expected is 33%, with the rest being oxygen.[38] Finally, it was suggested that about 18% surface concentration of titanium is reasonable for clean titanium in the normal environment.[39] High-resolution analysis of Ti2p peaks permitted to conclude that titanium observed on T and V surfaces is present in four oxidation states: Ti(0), Ti(+II), Ti(+III), and Ti(+IV) on polished samples. This is consistent with the commonly admitted structure of passivated layer on titanium: the metal is covered by a mixed layer of TiO and Ti_2O_3 compounds and TiO_2 layer grown at the top of the surface. For EE and SB samples, the only

TABLE II. The Atomic Concentration (%) of the Element Measured by XPS after the Different Treatments

	Pure Titanium					Stainless Steel					Ti6Al4V				
	P	EE	EE	SB	SB	P	EE	EE	SB	SB	P	EE	EE	SB	SB
Level		0	1	0	1		0	1	0	1		0	1	0	1
C 1s	68.37	53.50	66.38	52.59	44.70	65.51	38.06	50.41	36.11	39.94	70.32	55.84	56.50	46.05	54.10
O 1s	22.51	33.14	24.75	29.93	34.27	25.89	39.99	32.64	37.98	33.87	21.41	27.41	29.41	32.18	26.76
Ti 2p	3.64	6.41	0.95	1.98	3.26						2.46	2.86	4.60	2.00	2.61
	(39.9)	(47.8)	(10.7)	(11.3)	(15.5)						(29.7)	(17.1)	(32.6)	(9.2)	(13.6)
Fe 2p						2.76	2.97	2.20	3.94	4.27					
						(32.1)	(13.5)	(13.0)	(15.2)	(16.3)					
N 1s	1.96	4.04	3.92	1.10	2.13	0.92	1.33	4.69	0.37	1.53	2.15	4.38	2.35	1.19	0.82
	(21.5)	(30.2)	(44.2)	(6.3)	(10.1)	(10.7)	(6.1)	(27.7)	(1.4)	(5.8)	(26.0)	(26.1)	(16.7)	(5.4)	(4.3)
Al 2p				9.45	12.70				13.15	13.59	1.33	6.57	3.64	12.32	12.13
				(54.1)	(60.4)				(50.7)	(51.9)	(16.1)	(39.2)	(25.8)	(56.6)	(63.4)
Ca 2p	0.79	0.90	1.16	1.62	0.49						0.56	1.07	1.23	1.46	0.37
	(8.6)	(6.8)	(13.1)	(9.3)	(2.3)						(6.8)	(6.4)	(8.7)	(6.7)	(1.9)
Si 2p	1.62			1.28	1.58	2.41	5.07	3.54	4.72	2.23	1.77			2.97	1.81
	(17.8)			(7.3)	(7.5)	(28.0)	(23.1)	(20.9)	(18.2)	(8.5)	(21.4)			(13.6)	(9.5)
S 2p	1.11			2.05	0.88									1.82	1.40
	(12.2)			(11.8)	(4.2)									(8.4)	(7.3)
Zn 2p		0.74	0.32				0.62	0.74				0.38	0.61		
		(5.5)	(3.6)				(2.8)	(4.4)				(2.3)	(4.3)		
Cu 2p		0.45	0.67				1.61	0.58				0.42	0.50		
		(3.4)	(7.6)				(7.3)	(3.4)				(2.5)	(3.5)		
Cl 2p		0.82	1.85				1.23	0.46				1.08	1.16		
		(6.1)	(20.9)				(5.6)	(2.7)				(6.4)	(8.2)		
Cr 2p						1.04	4.34	1.00	1.30	1.69					
						(12.1)	(19.8)	(5.9)	(5.0)	(6.4)					
P 2p						1.14	2.97	3.39	2.03	2.29					
						(13.3)	(13.5)	(20.0)	(7.8)	(8.7)					
Mn 2p						0.33	1.82	0.36	0.42	0.58					
						(3.8)	(8.3)	(2.1)	(1.6)	(2.2)					

Numbers in Bracket: after deduction of the carbon and oxygen components.

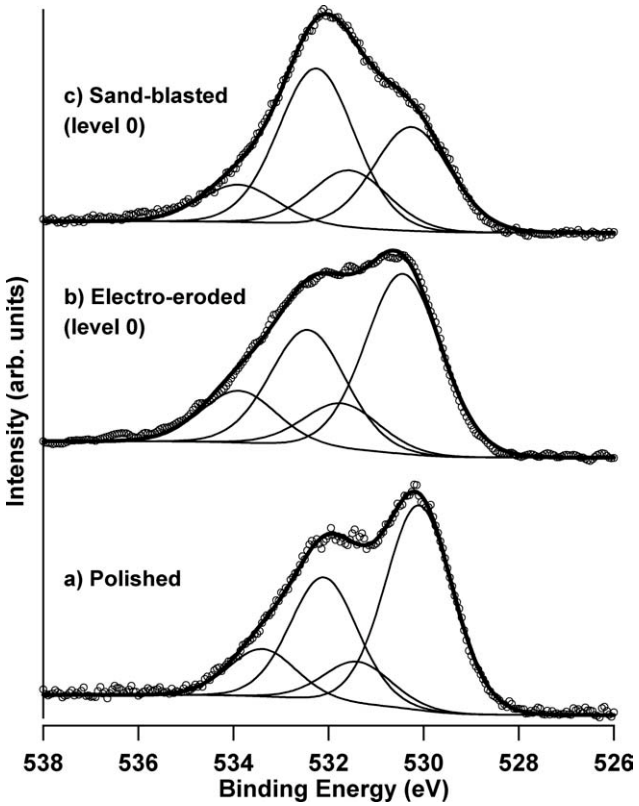

FIGURE 2. Variation of O1s high resolution spectra according to elaboration process: (a) polished, (b) electro-eroded, and (c) sand-blasted samples.

oxidation state detectable with the XPS is Ti(+IV). This shows that the process induces a growth of the oxide layer and that this oxide layer is thicker than the 9 nm probing depth of the XPS technique. For all conditions, the surface can be mainly considered as TiO_2 surface and the chemical environment of oxygen will determine the extreme surface chemistry. Contact angle value is a common surface parameter to investigate cell adhesion triggered by hydrophilicity. Unfortunately, our set of samples arises from various elaboration protocols that modify morphology (topography and roughness) as well as chemical contamination. Such characteristics are known to strongly influence contact angle values. Then, it becomes hard to determine a wettability parameter relevant for all samples and reflecting only the hydrophilicity of each sample. As a consequence, we decided to investigate oxygen ratios, derived from XPS measurements, as an indirect probe of the surface hydrophilicity. As seen in Table II, oxygen is the most abundant element at the surface of each sample if carbon due to contamination is not taken into account. If chemistry of surfaces plays a role on the AP, we can assume that chemical states of oxygen at the surface will be an important parameter. High-resolution spectra of O1s have been acquired on our spectrometer and the O1s envelope has been peak-fitted into four components. The first is related to oxygen in an oxide form (530.2 $\pm$ 0.2 eV), the second to hydroxide groups (531.5 $\pm$ 0.2 eV), the third to organic oxygen (O=C bonds, 532.3 $\pm$ 0.2 eV), and the last to water physically adsorbed and O—C organic contamination (533.5 $\pm$ 0.3 eV). The variation of lineshapes with surface preparation on T can be seen in Figure 2. The strong variations in atomic percentage of each component is due to contamination arising from manipulation as well as variation of oxide and hydroxide layer due to the process (see Table III).

Cell morphology

The human osteoblasts developed well and displayed a classical polygonal shape with filopodes on all the surfaces except on the coarse EE I ones (IE1) where the cells appeared damaged. The cells adhered and spread more on smoother EE and SB surfaces (VE0, TE0, IE0 and VS0, TS0, IS0, respectively) than on rougher ones (VE1, TE1, IE1 and VS1, TS1, IS1, respectively). On polished surfaces (VP, TP, IP), the cells attained confluence after 7 days irrespective of the material (Fig. 3). It was not the case on EE and SB surfaces. After 14 days, a confluent cell layer covering an extracellular matrix was observed on all the samples except on the coarse EE ones (VE1, TE1, IE1), where rare extracellular matrix was visible. After 21 days, cells formed a

TABLE III. Percentage of the Three Oxygen Species on the Surfaces

	Ox1: Oxide	Ox2: Hydroxyl	Ox3: Organic O2	Ox4: Water	Ox2/Ox1	OX3/Ox1	Ox4/Ox1
TP	35.02	16.71	31.58	16.69	0.48	0.90	0.48
TS0	21.46	22.41	32.31	15.05	1.04	1.51	0.70
TS1	25.93	14.9	29.34	9.227	0.57	1.13	0.36
TE0	33.77	26.12	14.1	21.25	0.77	0.42	0.63
TE1	5.98	22.62	44.88	19.99	3.78	7.51	3.34
VP	25.36	14.29	44.59	15.76	0.56	1.76	0.62
VSO	20.81	25.66	27.73	14.67	1.23	1.33	0.70
VS1	23.43	14.29	31.97	19.02	0.61	1.36	0.81
VE0	22.96	25.55	28.55	17.54	1.11	1.24	0.76
VE1	37.88	21.54	26.63	11.81	0.57	0.70	0.31
IE0	15.89	73.51	1.127	9.478	4.63	0.07	0.60
IE1	25.44	47.67	18.48	8.407	1.87	0.73	0.33
IP	48.04	22.15	18.21	11.6	0.46	0.38	0.24
IS0	42.47	31.02	16.15	10.37	0.73	0.38	0.24
IS1	42.8	23.52	19.93	13.75	0.55	0.47	0.32

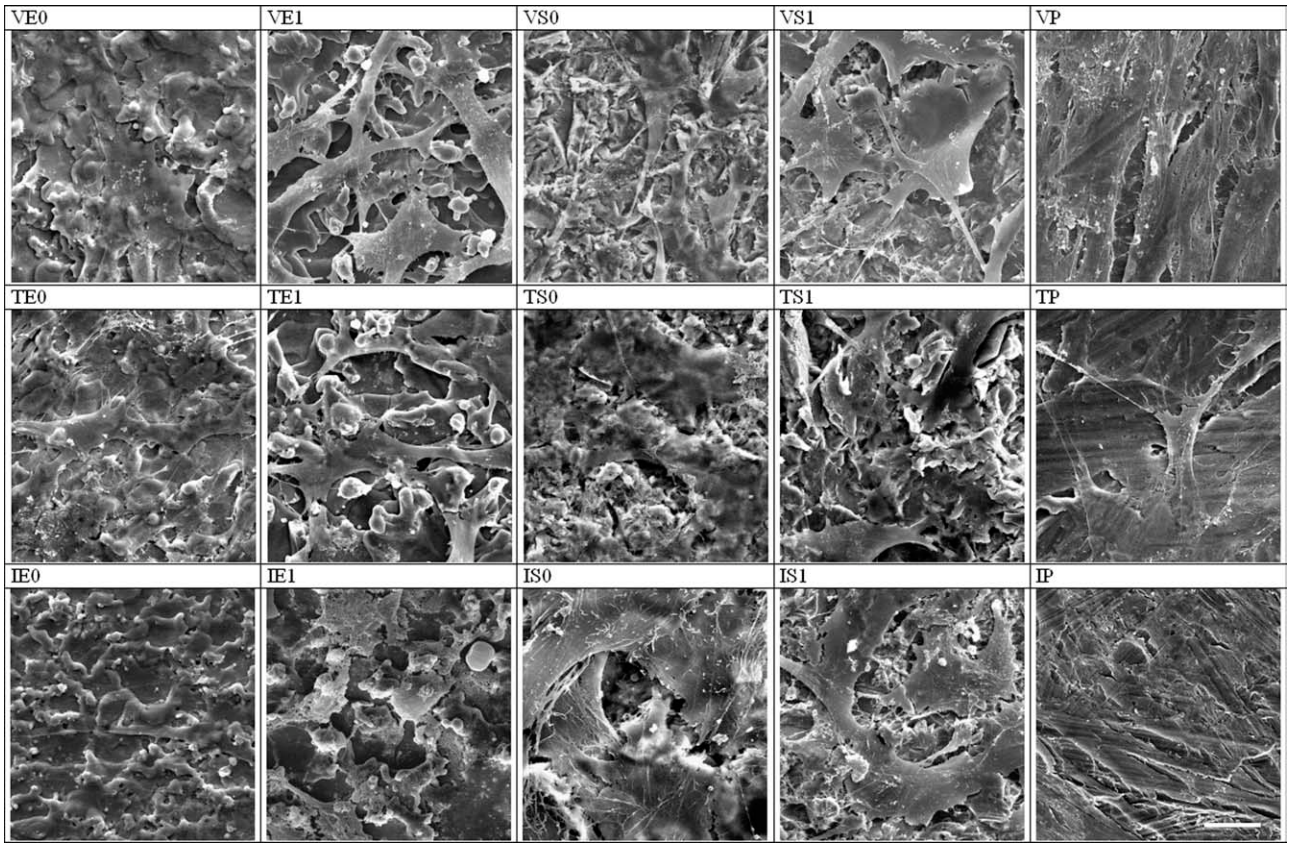

FIGURE 3. Scanning electron micrographs of cells after 7 days on pure titanium, Ti6Al4V and stainless steel EE, SB, and polished surfaces (bar = 30 μm). The human osteoblasts developed well and displayed a classical polygonal shape with filopodes on all the surfaces except on the coarse EE stainless steel ones (IE1) where the cells appeared damaged. The cells adhered and spread more on smoother EE and SB surfaces (VE0, TE0, IE0 and VS0, TS0, IS0, respectively) than on rougher ones (VE1, TE1, IE1 and VS1, TS1, IS1, respectively). On polished surfaces (VP, TP, IP), the cells attained confluence after 7 days whatever the material.

confluent layer on all the substrates except IE1 and VE1 (data not shown).

Statistical analysis of adhesion

To more specifically analyze the relative effects of material, process, or roughness amplitude on human osteoblast adhesion, we proceeded to different analysis of variance. First, to demonstrate statistically if the surface composition analyzed by XPS had an influence on cell response, we proceeded to a correlation study between the AP and the element percentages. Carbon and oxygen components are excluded from this correlation (Table II) as the first arises from organic contamination and the second will be analyzed in a specific procedure based on oxygen high-resolution components ratios (Table III). The raw atomic quantification has been completed by the ratio of each component according to the oxide one for statistical calculation and normalization purpose. No correlation was found between AP and element concentration (Fig. 4) and critical p values lay between $p = 0.1$ and 0.7 meaning that correlation was not significant at the usual level of 0.05. Same conclusions were made between AP and oxide ratios with a p value always greater than 0.3 (Fig. 5).

Second, we proceeded to the analysis of variance of the relative effects on AP of the three materials (V, T, or S), the two processes (sandblasting and electro-erosion), and the two different amplitude roughnesses. Figure 6 represents the mean effect for all these parameters. The results of this analysis of variance are presented on the Table IV. First, the effect of materials alone is not significant. The three materials, after sandblasting or electro-erosion, have no statistical influence on the cellular adhesion. Second, the roughness amplitude, independently of the process, has also no influence on the cellular adhesion: roughness amplitude is not an intrinsic parameter of adhesion. Third, on the contrary, the process alone has a significant effect on adhesion ($p = 0.0218$). Additionally, it exists a very high interaction ($F = 22$) between roughness amplitude and the elaboration process.

The Table V shows that this interaction is negative whatever the material: for the EE surfaces, AP is better for low roughness and on the contrary for the SB surfaces, AP is better for the high roughness amplitude.

As surfaces can be chemically modified by the electro-erosion or the sandblasting process, we analyzed the influence of materials nature on polished surfaces. We processed to an analysis of variance with one dimension (surface

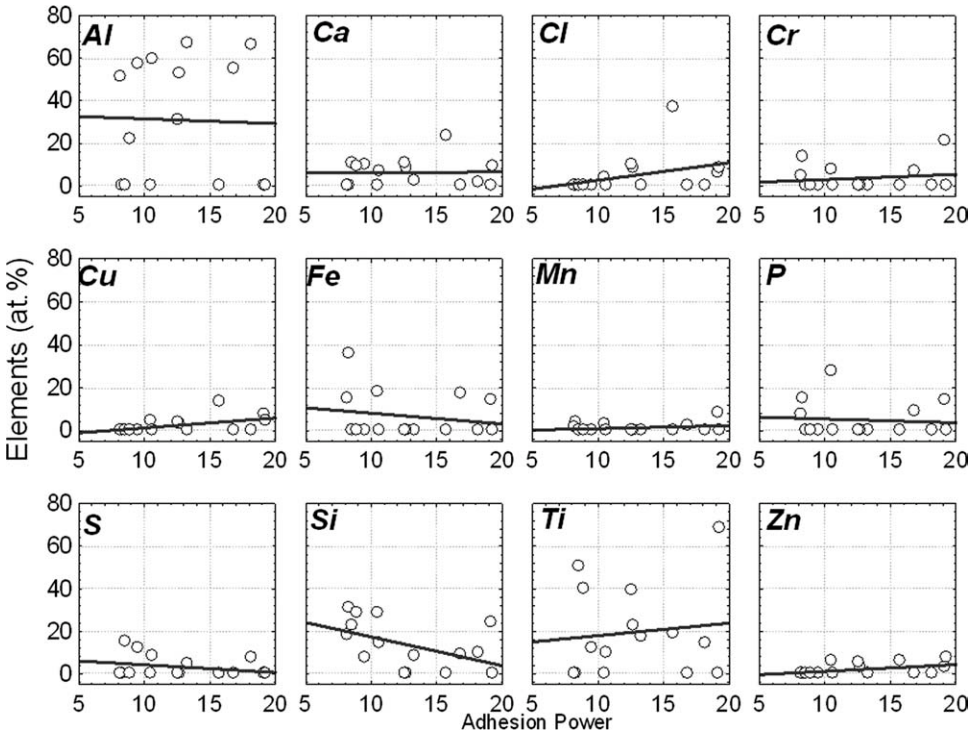

FIGURE 4. Correlation between Adhesion Power (AP) and element percentage calculated from XPS analysis of surfaces but after deduction of carbon and oxygen components.

process) and three levels (materials). Again, we did not demonstrate any effect on cellular adhesion of materials composition after polishing considering the low value of F ($F = 0.54$) and the probability associated ($p = 0.5857$). This one-dimension analysis of variance on polished surfaces confirmed that T, I, and V have the same biocompatibility.

Roughness analysis

As shown in Table I, the choice of appropriate process parameters used for electro-erosion and sandblasting allowed us to produce approximately the same Ra for the two levels of roughness. The number of peaks was lower for the higher level of roughness and the autocorrelation length increased with the roughness level. This remark was valid for the two processes. However, we have statistically demonstrated that AP was better for the low roughness amplitude on the EE surfaces and inversely for the SB surfaces, this effect being material-independent. This material independence means that only process plays a role in this effect. Consequently, we must find a roughness parameter that increases with roughness level (or decreases) for the SB surfaces and inversely decreases (or increases) for the EE ones that is characterized in the ANOVA by the value of the interaction between the level of roughness and the process. To find the parameters that could explain this inversion, 75 roughness parameters (amplitude, spectral, or fractal ones) were computed and analysis of variance were performed to find the parameters that statistically get the best interaction between the level of roughness and the process. We found only one parameter, the ratio of inflexion points or G parameter that got the higher interaction with roughness, process or the association of the two and consequently could explain this inversion ($F = 262$, $p < 0.0001$) (Table VI). None of the other 74 roughness parameters could explain this inversion (Fig. 7). The F value of the effect of material was not significant meaning that the effect of the number of inflexion points did not depend on the material itself but only on the process and on the roughness amplitude.

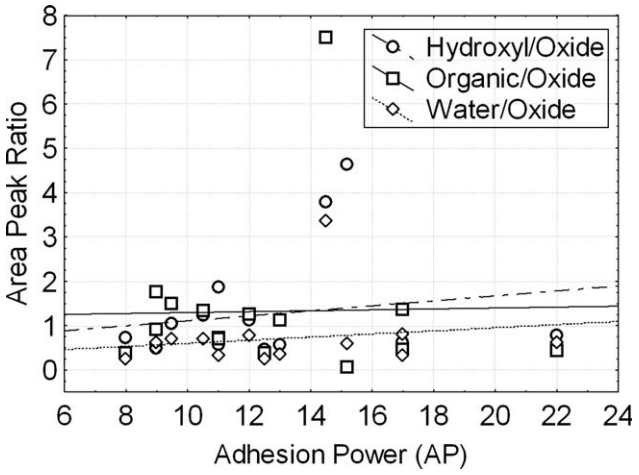

FIGURE 5. Correlation between adhesion power (AP) and oxygen species ratios calculated from XPS analysis of surfaces.

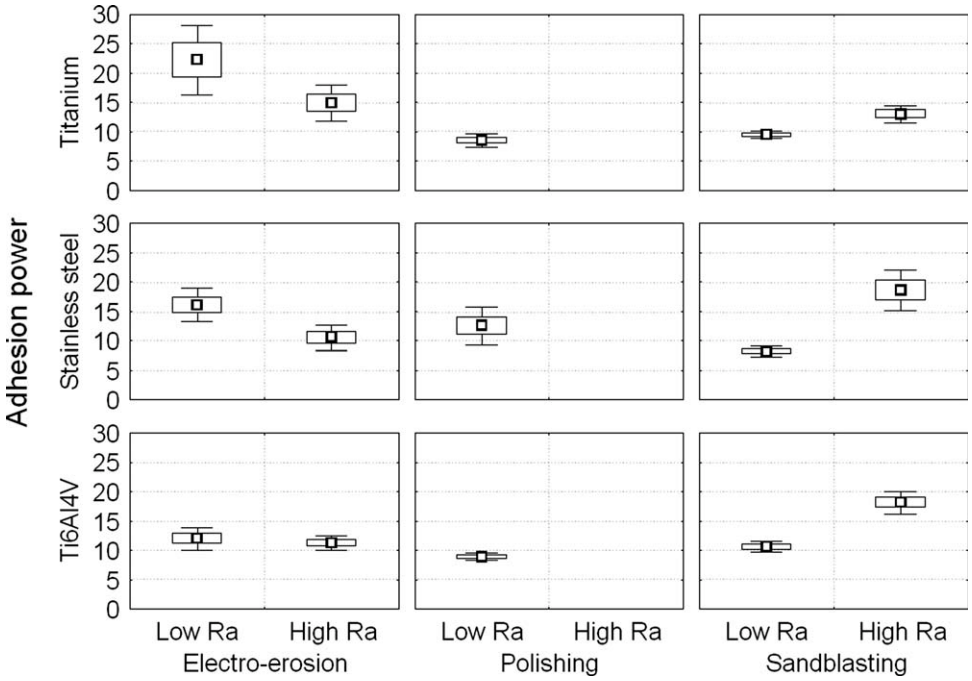

FIGURE 6. Mean effect of process and materials on adhesion power (AP).

DISCUSSION

Our objective was to determine by a statistical approach whether between surface chemistry (material nature) and surface topography (roughness amplitude, elaboration process) has the highest influence on human osteoblast adhesion.

Chemistry effect

The morphological observation of cells demonstrated rare differences between materials except on coarse IE1 samples where the cells appeared damaged. This can be related to previous studies made on I substrates showing that when compared with titanium-based substrates, the adhesion and proliferation of cells was lower or equal on S than on T or V.[27,40–42] However, these experiments concerned polished or SB substrates. In our case, we observed signs of corrosion only after coarse electro-erosion of I. Morais et al. have demonstrated that the I corrosion products above certain concentration may disturb the normal behavior of osteoblastic cells and could at 1% result in cell death.[43] Thus, in our experiment, the coarse electro-erosion process should have induced a weakness of the surface, the formation of some pits of corrosion and the release of corrosion products at the origin of the observed damages. Nevertheless, it has been difficult to attribute this effect to a single element present at the surface. On the contrary, we noted that the fine electro-erosion does not seem to have any adversary effect, demonstrating that it exists as a threshold in energy applied by the EE process that should not be overtaken.

Our statistical analysis demonstrated that there was no significant effect of the material composition on the AP as well on SB and EE samples as on polished ones. This would mean that the chemical composition has a low impact on adhesion. These results are slightly contradictory with the observed cellular damages observed on coarse IE1 substrates. However, in this case, we have a concomitant influence of process with material since the cellular damages are observed only after coarse EE.

Some elements appear to be increased in surface as function of the process used. For example, the C1s percentage is largely increased by polishing compared to EE and SB although the Ti 2p is comparable for the three different processing methods. This is in accordance with the

TABLE IV. Analysis of Variance of the Relative Effects on AP of the Three Materials (Materials), the Two Processes (Process), and the Two Different Roughness Amplitude (Roughness)

Source	DF	Type III SS	Mean Square	*F* Value	Pr > *F*
Material	2	87	43	1.09	0.3398
Roughness	1	61	61	1.53	0.2178
Process	1	216	216	5.36	0.0218
Process × Roughness	1	903	903	22.34	<0.0001

TABLE V. Mean values of Adhesion Power for the Two Roughness Amplitude Levels of Electro-Erosion and Sandblasting Processes Irrespective of the Material

Process	Roughness Amplitude	Number of Measurements	Adhesion Power
Electro-erosion	Level 0	45	16.60
Electro-erosion	Level 1	51	13.06
Sandblasting	Level 0	27	9.44
Sandblasting	Level 1	45	15.65

TABLE VI. Analysis of Variance of the Relative Effects on G of Materials (the Three Materials), Process (the Three Processes), and Roughness (the Two Different Roughness Amplitudes)

Source	DF	Type III SS	Mean Square	*F* Value	Pr > *F*
Material	2	0.00038	0.00019	1.00	0.3678
Process	1	0.01036	0.01036	53.2	<0.0001
Roughness	1	0.02138	0.02138	109.9	<0.0001
Process × Roughness	1	0.05103	0.05103	262.5	<0.0001

literature.[38] High-resolution XPS gives the opportunity to peak-fit O1s spectrum into components attributed to oxide, hydroxide, or oxygen arising from water molecules. The ratio between oxygen components should lead to different hydrophilicity and charges when surfaces are immersed in culture medium. As for material composition, there was no significant effect of oxygen components ratio on the AP (Fig. 5). This is another argument to say that early stage adsorption of biomolecules is preponderant and screens variations of surface chemistry towards cell adhesion. Finally, the absence of correlation between cell adhesion and the elements quantified by XPS at the material surface confirmed that the surface chemistry of metallic materials is not the main parameter influencing cell response. These results also confirmed the ability of proteinaceous coating adsorbed from the serum to translate various surface chemistries into a layer favorable for cell adhesion.

Topography effect

These results are coherent with our previous *in vitro* experiments with gold–palladium coated surfaces[6] and those obtained by Hacking et al.[23] that demonstrated the relative major effect of roughness versus chemistry on bone cell adhesion and tissue response. We have also demonstrated that

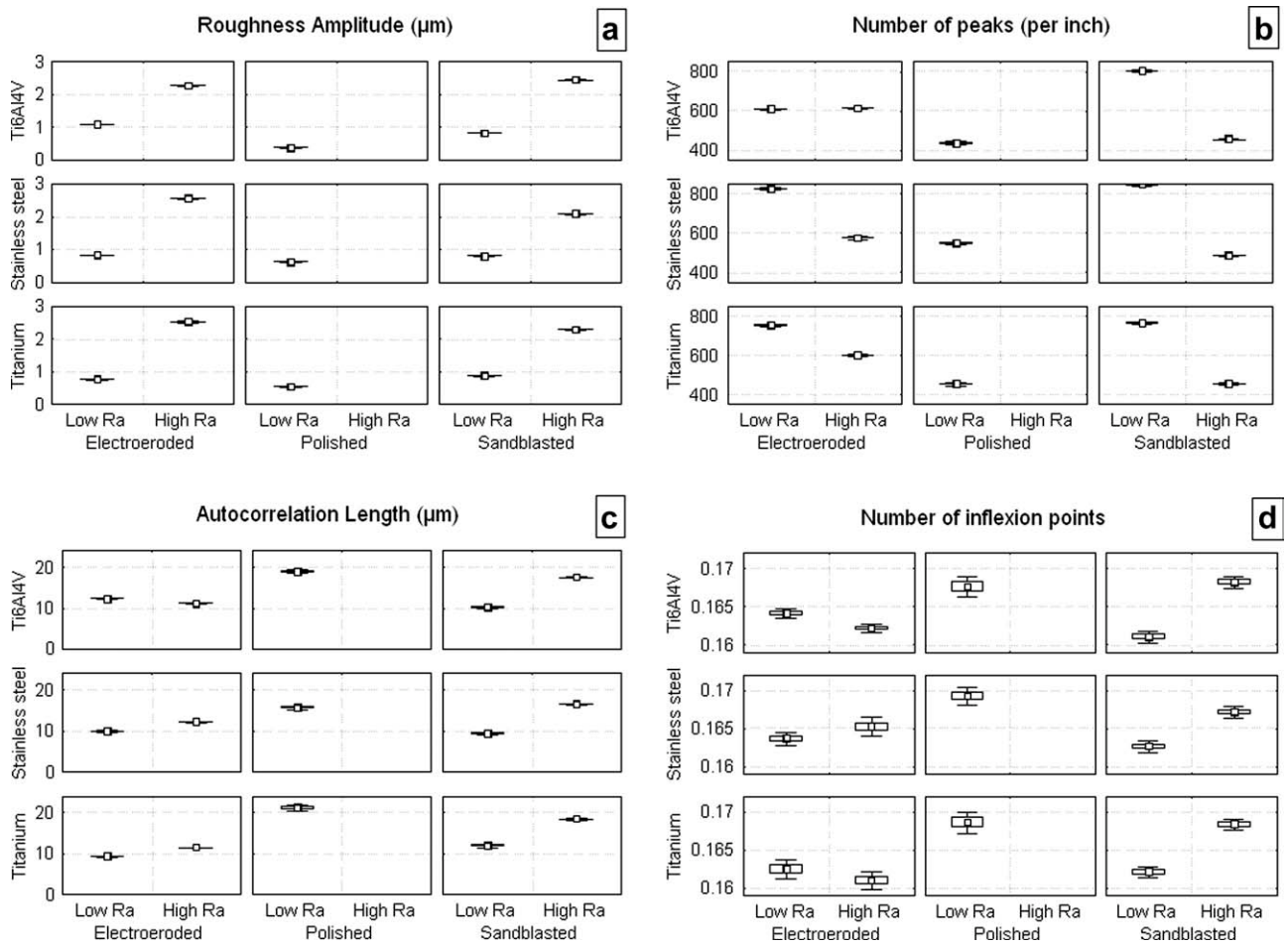

FIGURE 7. Mean effect of processes and materials on roughness amplitude (a), number of peaks (b), autocorrelation length (c), and number of inflexion points (d).

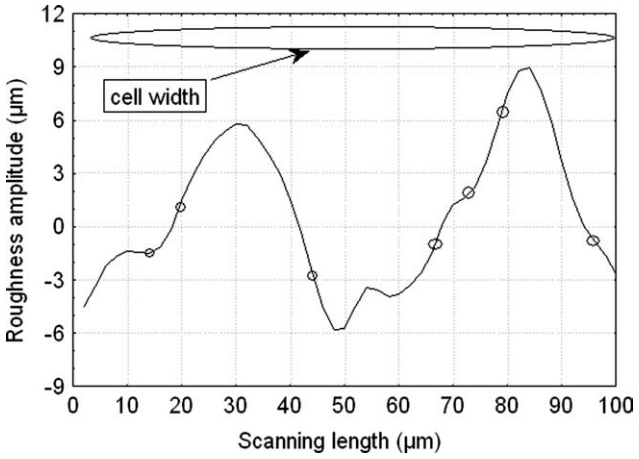

FIGURE 8. Profile of EE stainless steel surfaces with high amplitude (IE1). The cell width is illustrated and the inflexion points are visualized by circles.

the roughness amplitude is not an intrinsic parameter of adhesion. More precisely, we have shown on Ti samples that the order parameter is the roughness parameter that better discriminate adhesion.[36,44] Lower the order, higher the AP.

As neither the surface chemistry or roughness amplitude appears to have any influence alone on cell adhesion, the main influencing parameter is definitely the elaboration process used to produce the topography. Moreover, this process has a very high interaction with roughness amplitude meaning that the level of roughness (fine or coarse) has different effect if the surface is obtained by electro-erosion, sandblasting, or polishing. For EE surfaces, adhesion is better for lower roughness amplitude and for SB surfaces, adhesion is better for higher roughness amplitude. To explain this, we did search a roughness parameter that increased between fine and coarse SB surfaces and inversely decreased for EE ones. We found that the number of inflexion points was the parameter that got the higher interaction with roughness, process or the association of the two. One question to elucidate is why did the two processes (electro-erosion and sandblasting) give different numbers of inflexion points for different amplitude roughness levels. Concerning the electro-erosion process, we propose the following hypothesis. To obtain a higher roughness amplitude by electro-erosion, we need to increase the intensities on the electrode of the electro-erosion tool machine. Droplets become bigger, but they keep the same morphology.[32,44] As a consequence, the number of inflexion points that characterizes, briefly speaking, the reunion of two droplets, will decrease with intensity and consequently with roughness amplitude.

Concerning the sandblasting effect, another hypothesis is proposed. To obtain a higher roughness amplitude by sandblasting, we need to increase the size of the particles used for sandblasting (400 μm rather than 120 μm). A particle of 400 μm will plastically deform more adjacent grains than a particle of 120 μm. Then the number of deformed slip plans will be higher with a particle of 400 μm than with a particle of 120 μm and will further increase the number of inflexion points. As it could be observed from the calculated number of peaks, a cell will see about one or two peaks under itself. On the contrary, it will see about seven inflexion points under itself since the length between inflexion points is about 6 μm (Fig. 8). Finally, the cells seem to adhere better when the number of inflexion points increases. This could be related to the hypothesis proposed by Curtis and Clark who proposed that the cells react to discontinuities. A discontinuity has been defined on the biological point of view as a radius of curvature less than the average length of the distance part of the sensing elements that control cell movement.[45] Animal cells contain a cytoskeleton that is a network of protein filaments extending through the cell cytoplasm like actin filaments. Actin filaments are broken down and elongated constantly in live cells. The front edge of cells, the lamellipodia, contains actin microspikes. With these spikes, the cell probe the substrate surface for suitable attachment places after which focal adhesions and mature actin fibers are formed.[46] Thus these microspikes are likely able to sense the presence of peaks but also inflexion points in the relief of substrate surface.

As cells conform or attach to topography, some receptors would be subject to variable degrees of deformation or even compression. Concave surface will lead to compression while convex surfaces would cause tension.[47] These forces applied on the actin cytoskeleton will result in rearrangement of these filaments that will further modify cell adhesion, proliferation and differentiation. These conclusions mainly derived from studies on anisotropic surfaces presenting grooves or pits are certainly also applicable to discontinuities present on isotropic rough surfaces like those tested in this article as inflexion points can be considered as transitions between concave or convex part of the topography.

CONCLUSIONS

The comparison of long-term adhesion of human osteoblasts on I, V, and T substrates processed by electro-erosion, sandblasting, or polishing and presenting a fine or a coarse level of roughness demonstrated a good adhesion on all the substrates except on coarse IE1 substrates. These later displayed a corrosion phenomenon certainly at the origin of the cellular damages observed.

By the analysis of variance of more than 2500 data, we demonstrated that between surface chemistry (material nature) and surface roughness (roughness amplitude, elaboration process), the later was the parameter having the main statistical influence on long-term adhesion of human osteoblasts. Moreover, no correlation was observed between AP and the surface elements percentages determined by XPS demonstrating that the surface chemistry was not an influencing parameter for long-term adhesion. Therefore, we analyzed deeper the influence of surface topography on cell adhesion. The roughness amplitude was shown to have a very high interaction with the elaboration process meaning that the level of roughness had different effects on cell adhesion if surface was obtained by electro-erosion, sandblasting, or polishing. A new roughness parameter, the number of inflexion points, was found to increase between fine

and coarse SB surfaces and inversely decrease for EE ones, like AP. As the inflexion points can be identified by cells as discontinuities and since the discontinuities are known to be the influencing surface elements for cell adhesion, the G parameter can be considered as one pertinent parameter for describing the topography influence on long-term adhesion. Thus, more the inflexion points, more the discontinuities, higher the long-term adhesion.

APPENDIX: DETERMINATION OF THE NUMBER OF INFLEXION POINTS (G)

The algorithm was developed by on of the authors (M. Bigerelle).

An inflexion point is a point on a curve at which the curvature changes sign. The curve changes from being concave upwards (positive curvature) to concave downwards (negative curvature) or vice versa.

The main problem consists in counting the number of inflexion points. Four adjacent points are taken. From these four points, we calculate a third degree polynomial function:

$$z = a_1x^3 + a_2x^2 + a_3x + a_4$$

.

We must then have $\frac{d^2z}{d^2x} = 6a_1x + 2a_2$ that is equal to zero and changes sign.

In fact, we get an inflexion point between (x_{i+1},z_{i+1}) and (x_{i+2},z_{i+2}) if one of the two following conditions are met:

Condition 1: $6a_1x_{x+1} + 2a_2 > 0$ and $6a_1x_{x+2} + 2a_2 < 0$
Condition 2: $6a_1x_{x+1} + 2a_2 > 0$ and $6a_1x_{x+2} + 2a_2 > 0$

By varying i from 1 to N - 3 (N is the number of points of the profile), the number of inflexion points n is counted and normalized to the number of points of the profile: $g = \frac{n}{N-3}$ that represents the ratio of inflexion points.

ACKNOWLEDGMENTS

The authors would like to thank B. Noël and I. Loison for their technical assistance in cell culture experiments and P. Fioux for XPS analysis.

References

1. Wennerberg A, Hallgren C, Johansson C, Sawase T, Lausmaa J. Surface characterization and biological evaluation of spark-eroded surfaces. J Mater Sci Mater Med 1997;8:757–763.
2. Vercaigne S, Wolke JGC, Naert I, Jansen JA. Histomorphometrical and mechanical evaluation of titanium plasma-sprayed-coated implants placed in the cortical bone of goats. J Biomed Mater Res 1998;41:41–48.
3. Cooper LF. A role for surface topography in creating and maintaining bone at titanium endosseous implants. J Prosthet Dent 2000;84:522–534.
4. Gotfredsen K, Berglundh T, Lindhe J. Anchorage of titanium implants with different surface characteristics: An experimental study in rabbits. Clin Implant Dent Rel Res 2000;2:120–128.
5. Anselme K. Osteoblast adhesion on biomaterials. Biomaterials 2000;21:667–681.
6. Bigerelle M, Anselme K, Noël B, Ruderman I, Hardouin P, Iost A. Improvement in the morphology of surfaces for cell adhesion: A new process to double human osteoblast adhesion on Ti-based substrates. Biomaterials 2002;23:1563–1577.
7. Boyan BD, Lohmann CH, Dean DD, Cochran DL, Schwartz Z. Mechanisms involved in osteoblast response to implant surface morphology. Annu Rev Mater Res 2001;31:371.
8. Lange R, Lüthen F, Beck U, Rychly J, Baumann A, Nebe B. Cell-extracellular matrix interaction and physico-chemical characteristics of titanium surfaces depend on the roughness of the material. Biomol Eng 2002;19:255–261.
9. Deligianni DD, Katsala N, Ladas S, Sotiropoulou D, Amedee J, Missirlis YF. Effect of surface roughness of the titanium alloy Ti-6A1-4V on human bone marrow cell response and on protein adsorption. Biomaterials 2001;22:1241–1251.
10. Anselme K, Bigerelle M, Noël B, Lost A, Hardouin P. Effect of grooved titanium substratum on human osteoblastic cell growth. J Biomed Mater Res A 2002;60:529–540.
11. Ruardy TG, Schakenraad JM, Van der Mei HC, Busscher HJ. Adhesion and spreading of human skin fibroblasts on physicochemically characterized gradient surface. J Biomed Mater Res 1995;29:1415–1423.
12. Scotchford CA, Cooper E, Leggett GJ, Downes S. Growth of human osteoblast-like cells on alkanethiol on gold self-assembled monolayers: The effect of surface chemistry. J Biomed Mater Res 1998;41:431–442.
13. Zreiqat H, Howlett CR. Titanium substrata composition influences osteoblastic phenotype: In vitro study. J Biomed Mater Res 1999;47:360–366.
14. Lee TM, Chang E, Yang CY. Attachment and proliferation of neonatal rat calvarial osteoblasts on Ti6Al4V: Effect of surface chemistries of the alloy. Biomaterials 2004;25:23–32.
15. Keselowsky BG, Collard DM, Garcia AJ. Surface chemistry modulates focal adhesion composition and signaling through changes in integrin binding. Biomaterials 2004;25:5947–5954.
16. Zreiqat H, Valenzuela SM, Nissan BB, Roest R, Knabe C, Radlanski RJ, Renz H, Evans PJ. The effect of surface chemistry modification of titanium alloy on signalling pathways in human osteoblasts. Biomaterials 2005;26:7579–7586.
17. Sherratt MJ, Bax DV, Chaudhry SS, Hodson N, Lu JR, Saravanapavan P, Kielty CM. Substrate chemistry influences the morphology and biological function of adsorbed extracellular matrix assemblies. Biomaterials 2005;26:7192–7206.
18. Tsukimura N, Kojima N, Kubo K, Att W, Takeuchi K, Kameyama Y, Maeda H, Ogawa T. The effect of superficial chemistry of titanium on osteoblastic function. J Biomed Mater Res A 2008;84:108–116.
19. Anselme K, Linez P, Bigerelle M, Le Maguer D, Le Maguer A, Hardouin P, Hildebrand HF, Lost A, Leroy J-M. The relative influence of the topography and chemistry of Ti6Al4V surfaces on osteoblastic cell behaviour. Biomaterials 2000;21:1567–1577.
20. Wieland M, Chehroudi B, Textor M, Brunette DM. Use of Ti-coated replicas to investigate the effects on fibroblast shape of surfaces with varying roughness and constant chemical composition. J Biomed Mater Res A 2002;60:434–444.
21. Anselme K, Bigerelle M. Effect of a gold-palladium coating on the long-term adhesion of human osteoblasts on biocompatible metallic materials. Surf Coat Tech 2006;200:6325–6330.
22. Meredith DO, Riehle MO, Curtis ASG, Richards RG. Is surface chemical composition important for orthopaedic implant materials? J Mater Sci-Mater Med 2007;18:405–413.
23. Hacking SA, Tanzer M, Harvey EJ, Krygier JJ, Bobyn JD. Relative contributions of chemistry and topography to the osseointegration of hydroxyapatite coatings. Clin Ortho Related Res 2002;405:24–38.
24. Lampin M, Warocquier-Clérout R, Legris C, Degrange M, Sigot-Luizard MF. Correlation between substratum roughness and wettability, cell adhesion, and cell migration. J Biomed Mater Res 1997;36:99–108.
25. Links J, Boyan BD, Blanchard CR, Lohmann CH, Liu Y, Cochran DL, Dean DD, Schwartz Z. Response of MG63 osteoblast-like cells to titanium and titanium alloy is dependent on surface roughness and composition. Biomaterials 1998;19:2219–2232.
26. Hallab NJ, Bundy KJ, O'Connor K, Moses RL, Jacobs JJ. Evaluation of metallic and polymeric biomaterial surface energy and surface roughness characteristics for directed cell adhesion. Tissue Eng 2001;7:55–71.

27. Ponsonnet L, Comte V, Othmane A, Lagneau C, Charbonnier M, Lissac M, Jaffrezic N. Effect of surface topography and chemistry on adhesion, orientation and growth of fibroblasts on nickel-titanium substrates. Mat Sci Eng C 2002;21:157–165.
28. Schweikl H, Müller R, Englert C, Hiller KA, Kujat R, Nerlich M, Schmalz G. Proliferation of osteoblasts and fibroblast on model surfaces of varying roughness and surface chemistry. J Mater Sci Mater Med 2007;18:1895–1905.
29. Wirth C, Grosgogeat B, Lagneau C, Jaffrezic-Renault N, Ponsonnet L. Biomaterial surface properties modulate in vitro rat calvaria osteoblasts response: Roughness and or chemistry? Mater Sci Eng C 2008;28:990–1001.
30. Ismail FSM, Rohanizadeh R, Atwa S, Mason RS, Ruys AJ, Martin PJ, Bendavid A. The influence of surface chemistry and topography on the contact guidance of MG63 osteoblast cells. J Mater Sci Mater Med 2007;18:705–714.
31. Anselme K, Bigerelle M. Statistical demonstration of the relative effect of surface chemistry and roughness on human osteoblast short-term adhesion. J Mater Sci Mater Med 2006;17:471–479.
32. Anselme K, Bigerelle M. Modelling approach in cell/material interactions studies. Biomaterials 2006;27:1187–1199.
33. Bigerelle M, Anselme K. A kinetic approach to osteoblast adhesion on biomaterial surface. J Biomed Mater Res A 2005;75: 530–540.
34. Bigerelle M, Anselme K. Bootstrap analysis of the relation between initial adhesive events and long-term cellular functions of human osteoblasts cultured on biocompatible metallic substrates. Acta Biomater 2005;1:499–510.
35. Anselme K, Bigerelle M, Noel B, Dufresne E, Judas D, Lost A, Hardouin P. Qualitative and quantitative study of human osteoblast adhesion on materials with various surface roughness. J Biomed Mater Res 2000;49:155–166.
36. Anselme K, Bigerelle M. Topography effects of pure titanium substrates on human osteoblast long-term adhesion. Acta Biomater 2005;1:211–222.
37. Bigerelle M, Anselme K. Statistical correlation between cell adhesion and proliferation on biocompatible materials. J Biomed Mater Res A 2005;72:36–46.
38. Morra M, Cassinelli C, Bruzzone G, Carpi A, Di Santi G, Giardino R. Surface chemistry effects of topographic modification of titanium dental implant surfaces: 1. Surface analysis. Int J Oral Maxillofac Implants 2003;18:40–45.
39. Morra M, Cassinelli C. Evaluation of surface contamination of titanium dental implants by LV-SEM: Comparison with XPS measurements. Surface and Interface Anal 1997;25:983–988.
40. Anselme K, Noel B, Hardouin P. Human osteoblasts adhesion on titanium alloy, stainless steel, glass and plastic substrates with same surface topography. J Mater Sci Mater Med 1999;10: 815–819.
41. Vrouwenvelder WCA, Groot CG, de Groot K. Histological and biochemical evaluation of osteoblasts cultured on bioactive glass, hydroxyapatite, titanium alloy and stainless steel. J Biomed Mater Res 1993;27:465–475.
42. Olivares R, Rodil SE, Arzate H. In vitro studies of the biomineralization in amorphous carbon films. Surf Coat Technol 2004; 177–178:758–764.
43. Morais S, Sousa JP, Fernandes MH, Carvalho GS, de Bruijn JD, Van Blitterswijk CA. Effects of AISI 316L corrosion products in in vitro bone formation. Biomaterials 1998;19:999–1007.
44. Bigerelle M, Anselme K, Dufresne E, Hardouin P, Lost A. An unscaled parameter to measure the order of surfaces. A new surface elaboration to increase cells adhesion. Biomol Eng 2002;19:79–83.
45. Curtis A, Clark P. The effect of topographic and mechanical properties of materials on cell behavior. CRC Rev Biocompatibility 1990;5:343–362.
46. Walboomers XF, Croes HJE, Ginsel LA, Jansen JA. Growth behavior of fibroblasts on microgrooved polystyrene. Biomaterials 1998;19:1861–1868.
47. Curtis ASG, Wilkinson C. Topographical control of cells. Biomaterials 1997;18:1573–1583.